



Zentuti, N. A. M., Booker, J. D., Bradford, R. A. W., & Truman, C. E. (2020). Probabilistic Structural Integrity: Methodology and Case-Study in the Creep Regime. *Materials at High Temperatures*, 37(2), 101-113. <https://doi.org/10.1080/09603409.2019.1709731>

Peer reviewed version

Link to published version (if available):
[10.1080/09603409.2019.1709731](https://doi.org/10.1080/09603409.2019.1709731)

[Link to publication record in Explore Bristol Research](#)
PDF-document

This is the author accepted manuscript (AAM). The final published version (version of record) is available online via Taylor & Francis at <https://www.tandfonline.com/doi/full/10.1080/09603409.2019.1709731>. Please refer to any applicable terms of use of the publisher.

University of Bristol - Explore Bristol Research

General rights

This document is made available in accordance with publisher policies. Please cite only the published version using the reference above. Full terms of use are available: <http://www.bristol.ac.uk/red/research-policy/pure/user-guides/ebr-terms/>

1

2

3

4

5

6

7

8

9

10

11

12

13

14

15

16

17

18

19

20

21

22

23

24

25

26

27

28

29

30

31

32

33

34

35

36

37

38

39

40

41

42

43

44

45

46

47

48

49

50

51

52

53

54

55

56

57

58

59

60

61

62

63

64

65

Probabilistic Structural Integrity: Methodology and Case-Study in the Creep Regime

N A Zentuti, J D Booker, R A W Bradford, C E Truman
Solid Mechanics Research Group, University of Bristol, United Kingdom

Abstract

This paper presents a methodology for conducting probabilistic assessments for structural integrity applications based on the Monte-Carlo method. This starts with the definition of the underlying procedure for assessing the failure mechanisms of interest, followed by the statistical modelling of the key input parameters, leading to the estimation of desired probabilities. A case-study assessing a plant component (the tubeplate) for creep-fatigue crack initiation using the R5 Volume 2/3 procedure was conducted to provide context and demonstrate the utilities of implementing a probabilistic framework. Expanding on previous work, this paper highlights the main areas of focus for the proposed probabilistic methodology: probabilistic representation of input parameters, correlations, treatment of loading uncertainties, conducting post-assessment sensitivity analyses, the extrapolation of assessment location probabilities to component-level and, thereafter, population-level estimates. Through presenting a case-study implementing the full probabilistic methodology, the aim is to promote wider application and acceptance within the international structural integrity community, and further development of the methodology and constituent methods.

Keywords: Structural integrity, probabilistic, Monte-Carlo, plant components, creep-fatigue

1. INTRODUCTION

Probabilistic structural integrity has been an active area of development in recent years, with high temperature applications (e.g. those examining metal creep failure) being driven by the need for examining uncertainties associated with in-service components. Historically, numerous codes, standards and pro-

*Corresponding author
Email address: nz9512@my.bristol.ac.uk (N A Zentuti)

cedures have been developed to assess in-service components for creep or creep-fatigue failures [1]. Chief examples are the American ASME III Subsection NH design code [2], the French RCC-MRx design codes [3], the BS7910 assessment procedure by the British Standards Institution [4] and the R5 procedure [5] developed by the UK power generation industry, which has been the major methodology applied to AGR components.

Currently, the use of probabilistic methods has been alluded to in some structural integrity codes and procedures including the R6 procedure (the low-temperature counterpart to R5), and the R5 Volume 4/5 (Appendix A7) procedure concerning creep-fatigue crack growth, though the extent of such guidance remains limited [6]. However, presently no formal advice is available for R5 Volume 2/3, which has recently prompted the creation of Appendix 15 (recently approved by the R5 Panel), which is intended to give some general, non-prescriptive advice. From a regulatory prospective, in the UK there are currently no allowances for use of probabilistic methods for nuclear structural integrity safety cases. As a result, the main proponents for probabilistic implementation have been from industry and academic stakeholders. The absence of explicit sanction for the use of probabilistics in nuclear structural assessments is a curious inconsistency since nuclear safety cases, more broadly, are intrinsically reliant upon probabilistic concepts. For example, the PSA (probabilistic safety assessment), ALARP (as low as reasonably practicable) and the dose-frequency staircase which are probabilistic in nature [7, 8].

Conventionally, the above mentioned codes and procedures describe calculations which are predominantly deterministic, which most commonly rely on conservatism to account for uncertainty, and consequently a number of complex issues are not formally considered [9]. Formally addressing these issues becomes unavoidable as plant components progress through their life expectancy, and the focus shifts from not only estimating the residual life whilst ensuring the highest level of safety, but also arguing for life extension in some cases. As a

result, the focus shifts towards quantifying failure probabilities, which fall beyond the purposes of traditional deterministic approaches, while probabilistic paradigms are well equipped for such applications.

Limited work has been conducted in the area of probabilistic high temperature structural integrity, a review of which can be found in [9]. Building on previous work [9, 10, 11, 12], this paper presents a complete, though non-exhaustive, methodology for the implementation of probabilistic methods at the various stages of assessing a plant component using well-established structural integrity codes or procedures. This methodology is intended to be divorced from any specific code or procedure and can be translated to any structural integrity application. The proposed methodology implements Monte-Carlo simulations (MCS) to estimate probabilities related to individual assessment locations. In essence, a MCS aggregates various sources of input uncertainty through a performance function (i.e. a structural integrity procedural calculation) to estimate the uncertainty in an output parameter, based on which probability estimates of interest can be computed. Due consideration is given to various issues: the statistical treatment of relevant material properties, sampling, inclusion of input parameter correlations, treatment of loading uncertainties and sensitivity analyses. The final components of the proposed methodology are concerned with estimating component-level probabilities which, in turn, can be translated to population-level estimates.

2. METHODOLOGY

2.1. The Probabilistic Approach

The MCS is applicable to complex applications where the inclusion of non-normal input parameters is needed [13, 14]. Given that the calculations required as part of most structural integrity procedures (creep-fatigue crack initiation being a good example) are typically complex, non-linear, multi-staged and may require numerical approximations (e.g. integration routines), the MCS is deemed

to be the only viable option for calculating probability estimates. In essence, a MCS strives to approximate the probability distribution of an output parameter based on the repeated computations of the input-output function (also called a *performance function*) using randomly generated combinations of the input variables, with the values going into these randomly generated combinations being sampled from probabilistic representations of the inputs (e.g. probability distributions). The performance function is defined by the underlying deterministic procedure, which for the case-study presented in this paper is prescribed by the R5 Volume 2/3 assessment procedure. Considering creep-fatigue crack initiation, a key probabilistic output is the probability of initiation (*PoI*) at a specific assessment location. To produce appropriate representations of the creep-fatigue damage distribution, a suitably large number of Monte-Carlo *trials* (typically $10^5 - 10^7$) must be computed. This puts a limitation on the applicability of MCS for computationally intensive calculations. For such cases a sampling strategy such as *latin-hypercube sampling* can aide in reducing the number of trials needed [15].

Latin-hypercube Sampling (LHS) is based on the principle that for each input parameter the samples going into the MCS must have equal probability. For instance, if an input parameter distribution is known then samples are determined by dividing the area under the PDF into portions of equal areas, which in fact represent equal probabilities of occurrence. This concept is depicted in Figure 1 for an arbitrary normal distribution. This ensures that even though there may be a relatively small number of samples, these are truly representative of the underlying distribution. A detailed account of the LHS strategy can be found in [16]. This sampling method relies upon all resulting combinations (i.e. MCS trails) having equal probability which is ensured by choosing the bins (i.e. the ranges of values) to have equal probability. Therefore, careful definition of the bins is crucial to the outcome of a MCS using LHS.

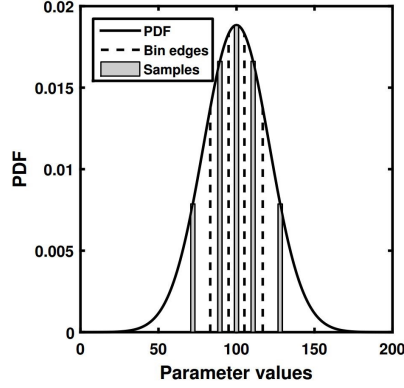


Figure 1: Example showing parameter samples having equal probabilities (5 samples obtained using the LHS approach) for an arbitrary normal distribution, with the samples being further apart (i.e. wider bins) towards the tails of the distribution.

2.2. Probabilistic Treatment of Input Parameters

Conventional deterministic calculations fail to make full use of the statistical information that could be inferred from available data. Scatter in test data may be attributed to a number of sources including: test procedures and equipment, data analysis methods and interactions between failure modes [17]. Lognormal distributions have been commonly adopted to statistically characterise various material data, especially for models where power laws are used [17, 9]. Furthermore, sampling of discrete data (i.e. histograms) may also be appropriate, for example, when dealing with uncertainties in loading parameters. Regardless of the application, for any given input parameter, it is encouraged that full use of the available data is made by choosing from the following options for input characterisation:

1. *Single value*: A parameter is fixed at a value believed to be appropriate (conservative perhaps), which is acceptable when very little data or understanding is available.
2. *Range of values*: This entails modelling the range of possible values as a flat (uniform) PDF. The limits of such a range would be based on experienced judgement and the available data.

3. *Probability distribution*: fitting one of many possible distribution types to the available data and using goodness-of-fit tests (e.g. χ^2) to decide which type is best suited. Typically, sample sizes ≥ 15 would be appropriate for this option [13], while for smaller data sets means and standard deviations can be calculated. Methods for fitting distributions are typically based on either the *linear regression method* [18, 13] or the *maximum likelihood method* [18, 9, 19].
4. *Histograms*: if no probability distribution is appropriate, then constructing a discreet representation of the available data, in the form of a histogram, may be more appropriate.

Sometimes the original data is not available, but a source may quote a mean and a standard deviation, or a 95% confidence limit. These suffice to define a two parameter probability distribution (e.g. normal or lognormal). If a parameter is assumed to follow a lognormal distribution, then its logarithmic value follows a normal distribution. The mean (μ) and standard deviation (σ_{Std}) of the latter normal distribution can be calculated based on the best estimate (BE) and lower-bound (LB) values which are commonly quoted in material property handbooks:

$$\sigma_{Std} = \frac{1}{CF} \log_{10} \left(\frac{BE}{LB} \right) \quad (1a)$$

$$\mu = \log_{10} (BE) \quad (1b)$$

where CF refers to a confidence factor which depends on the confidence limit associated with the LB. For example, if the LB is assumed to coincide with the 95% confidence limit, then CF is 1.6445 which is obtained by inverting the normal CDF.

2.3. Correlations between Probabilistic Inputs

The topic of characterising and incorporating correlations between the input parameters was discussed in detail in [11]. In essence, it was advised that no correlations need considering in the first instance when constructing a probabilistic

assessment, as conducting sensitivity analysis for an assessment without correlations can be used to narrow down the number of dominant parameters, the correlation between which might significantly influence the assessment results. After identifying which inter-parameter correlations would be most important, the degree of correlation may be based on judgement (e.g. choosing a value that would yield a conservative result when no relevant data is available), or based on experimental data. Correlations can be incorporated in an assessment using the *Gaussian copula* method [20, 21] to generate multivariate input samples which follow arbitrary PDFs and correlations. For the case-study the correlation between creep ductility and deformation was taken to be 54.5% (for more details on this specific correlation see [11]).

2.4. Sensitivity Analysis

Within the context of this work, sensitivity is a measure of the uncertainty in the probabilistic output (e.g. creep-fatigue damage) introduced by the various input conditions. In this work, sensitivity analysis was subdivided into two types of analyses determined by the subject input conditions:

1. *Stochastic input parameters:* e.g. those discussed in Sections 2.2. There exists various approaches to quantitatively measure the sensitivity of an output due to input parameter uncertainties [22, 23, 17], and four such approaches are summarised in [9].
2. *Modelling uncertainties;* these arise from the existence of competing assumptions and phenomenological representations of the failure mechanism (e.g. having various models to represent creep ductility, damage or deformation as functions of temperature and stress). These would be categorised as epistemic uncertainties, which arise from an initial lack of knowledge as to which models better represent the failure mechanisms. Assessing which model yields the better representation can only be done comparatively and with respect to experimental or inspection data. However, when constructing a probability assessment, the knowledge of whether the

output results are at all sensitive to which model used can be quite valuable. In which case, a purely comparative analysis contrasting the results obtained from using different models is initially sufficient.

The first category of input conditions typically considers uncertainties which are *aleatory* (i.e. random) in nature, whilst the latter type examines the sensitivity toward epistemic (i.e. systematic) uncertainties. Examples of implementing the above types of SA with reference to the tubeplate case-study are presented in Section 3.2.3.

2.5. Probabilities for Individual Assessment Locations

Given the results of a MCS for a single assessment location, probability estimates can be calculated based on a failure criterion that is prescribed by an assessment procedure. For instance, given a creep-fatigue crack initiation assessment, the probability of initiation is calculated as the probability of incurring a total damage greater than unity:

$$PoI = P(D_T \geq 1) \quad (2)$$

A probabilistic creep-fatigue calculation yields the total damage (D_T) as an uncertain output and the PoI can be estimated by calculating the fraction of the MCS trials which result in initiation given the failure criterion $D_T \geq 1$, thus giving $PoI = \frac{m}{N}$, where m is the number of initiations. Ultimately this is the preferred approach but requires a suitably large number of trials to capture the PoI within a decent resolution. The error associated with this PoI estimate can be estimated by considering that the number of crack failures (m) follows a binomial distribution [24]:

$$\epsilon = \frac{\sqrt{V(m)}}{E(m)} = \frac{\sqrt{NPoI(1-PoI)}}{NPoI} = \sqrt{\frac{1-PoI}{NPoI}} \quad (3)$$

where ϵ is the coefficient of variance, while $V(m)$ and $E(m)$ are the variance and mean of m respectively.

2.6. Component-Level Probability

Determining which assessment points are most likely to initiate first is crucial, but estimating a component-level probability of initiation (PoI_C) might be more consequential. It is assumed here that a PoI_C is interpreted as the probability of a shallow crack initiating *anywhere* within a component by the end of a predefined service history. Logically, this is greater than its equivalent for individual assessment points. A simple, and conservative, assumption is to assume that all assessment locations are *completely* independent of each other, in which case PoI_C can be calculated using [24]:

$$PoI_C = 1 - \prod_{a=1}^{A_T} (1 - PoI_a) \quad (4)$$

where PoI_a is associated with an assessment point a and A_T is the total number of assessment locations. In reality, for high reliability components this will be quite conservative as complete independence is not realistic. This consideration is especially important when correlations between the assessment locations (arising from both loading conditions and material properties) are crucial in estimating the overall initiation probability of a whole component. A similar argument can be made when a population of components (made from the same material and/or part of the same plant) are considered, as the probability estimates of components will be correlated, and these correlations are important for estimating population-level failures.

Accordingly, a more realistic estimate can be obtained by tracking all assessment locations in parallel as the component history is simulated through time. As a result, PoI_C is simply calculated as the fraction of the MCS trials which have led to at least one crack initiation across the whole component. In essence, this is a *weak-link* argument, which implies that a single point of failure (crack initiation in the case-study) is considered to mean failure of the entire component. What transpires from such analysis is that the PoI_C is dominated by the initiation of a small number of assessment points, which are usually the

points with the highest $PoIs$. As a result, a joint probability of initiation on the component-level (PoI_{JC}) can be estimated by tracking the dominant assessment locations. However, following this approach, which attempts to account for the interdependence between assessment locations, poses an issue: the non-dominant assessment locations (of which there might be a larger number than the dominant ones) need to be considered. These are the assessment locations which did not yield a quantifiable PoI given the resolution of the MCS. For example, if a MCS uses 1000 trials, non of which lead to initiation for a specific assessment location, the probability is not zero but rather smaller than the minimum PoI of 10^{-3} that this example MCS would be able to estimate. In practice, however, there maybe situations where the number of trials is taken to the limit of computational power available, in which case being able to estimate such a small PoI becomes challenging. To address this issue the following strategy is proposed:

1. Firstly, if an assessment yields zero failures by the end of the simulation, then it would be sensible, and conservative, to assume that at least one MCS trial leads to initiation (even though the results suggest otherwise) and therefore the PoI would have a default minimum of $1/N$.
2. Secondly, to incorporate this assumption in the PoI_C estimate, Eq 4 can be rewritten to separate the terms associated with the dominant from the non-dominant assessment locations:

$$PoI_C = 1 - \prod_{b=1}^{B_T} (1 - PoI_b) \prod_{c=1}^{C_T} (1 - PoI_c) \quad (5)$$

where B_T and C_T refer to the numbers of dominant and non-dominant assessment locations respectively, the sum of which is A_T . It is usually the case that $B_T < C_T$.

3. The product to the left (dominant terms) is estimated based on the weak-link argument put forward above, while the latter product is estimated based on assuming complete independence of the non-dominant terms:

$$PoI_C = 1 - (1 - PoI_{JC}) \left(1 - \frac{1}{N}\right)^{C_T} \quad (6)$$

2.7. Population-Level Estimates

A further metric which might be of interest is the number of components predicted to have at least one crack initiation given a population of such plant components, N_{TC} . A possible assumption may be that all components have the same PoI_C , which would imply that they all have the same material properties and have experienced the same severity of loading. Nevertheless, in practice that is rarely the case, and if the PoI_C is estimated for a single component which is considered bounding, then the estimated number of components having at least one crack (N_{CC}) would be conservative. It must be clarified that this estimation is uncertain rather than exact, as it follows a binomial distribution:

$$PoI_P = \binom{N_{CC}}{N_{TC}} PoI_c^{N_{CC}} (1 - PoI_c)^{N_{TC} - N_{CC}} \quad (7)$$

where PoI_P is the probability density of observing N_{CC} occurrences in the N_{TC} population. If this approach is too conservative, then component specific assessments can be conducted (i.e. estimating PoI_C for a number of identical components separately), but is inevitably onerous. As a result, if the components have differences, then the discussion becomes the same as for a single component with multiple assessment locations (see Section 2.6). A consideration that must be addressed in such case is whether the probability of at least one component developing a crack becomes dominated by the components with smaller individual $PoIs$, which would be the case if their numerical preponderance is sufficient. This is analogous to the discussion around Eq 5, as the product related to the non-dominant components becomes large due to their prevalence (i.e. $B_T \ll C_T$, but with reference to components rather than assessment locations).

2.8. Computational Deployment

Probabilistic assessments as described in this work are suited to implementation using general-purpose, high-level coding languages including Python, R and MATLAB, the latter of which was used. Various techniques that are common practice within these languages are suited for the application at hand. For

example, *vectorisation* is an efficient strategy which allows for the increase of number of trials without proportional increase in execution time. Using vectorisation, all trials are progressed through the simulated history simultaneously, which makes it slightly time consuming because some trials are computationally quicker than others. This is regarded as a small sacrifice given the improved efficiency relative to sequential calculations, and could be resolved with more complex algorithms. Moreover, there are three further attributes make these languages ideal. Firstly, they have numerous statistical libraries which have been thoroughly validated and in the public domain for years. Secondly, they provide a plethora of data visualisation tools, which are essential in conducting, reporting, presenting and independently verifying probabilistic assessments. Finally, they provide options for conducting parallel computations, which can be essential. Parallel computations can be done using CPU or GPU hardware, and the former was used in this work primarily for simplicity. However, when moving towards assessing multiple assessment locations with large MCS trials each ($\geq 10^6$) in parallel, then using a GPU (which is ideal for large array manipulations) may be more appropriate.

3. CASE-STUDY: THE TUBEPLATE COMPONENT

3.1. Background

This case-study was conducted to demonstrate the implementation of the probabilistic methodology presented in Section 2. The object of this case-study is a tubeplate (TP) boiler plant component which was assessed for creep-fatigue crack initiation. The TP is a cylindrical component which has 37 tubeholes, an FE representation of which is shown in Figure 2. Figure 3 shows a hysteresis cycle representing a typical loading cycle, where the start-of-dwell stress (σ_B , point B) is taken to be at an intermediate position in the hysteresis cycle, which is typical for a point near the surface of a tube bore. Point B is dictated by steady operation (i.e. power-producing) which can induce large temperature

260 differences between tubeholes, which result in large stress gradients, thus driv-
 ing creep-fatigue damage. The start-up transient (SU, Point A in Figure 3) is
 characterised by a compressive stress state whilst the reactor-trip (RT, Point C)
 typically induces a tensile stress on the surface of a tubehole [10]. The simulated
 history included 170 RT-SU loading cycles spanning a 30 year period. In total,
 265 this included approximately 19,000 steady-operation (SO) events, each of 100
 hours or less.

All input parameters deemed important were treated probabilistically and
 are summarised in Table 1. The TP is manufactured from 316H stainless steel
 270 forging, and the variabilities (i.e. data scatter) of key material properties were
 treated probabilistically using normal and lognormal distributions as discussed
 towards the end of Section 2.2. Loading uncertainties were also treated prob-
 abilistically, and this topic was examined in detail as part of related work. A
 more detailed account of the methods and results involved in predicting stresses
 275 (σ_{SO} , σ_{SU} and σ_{RT}) and metal temperatures (T_{SO} , T_{SU} and T_{RT}) based on
 historic plant data for the tubeplate can be found in [25, 10]. Thereafter, key
 results obtained from the probabilistic creep-fatigue assessment are presented
 in Section 3.2, including the *PoIs* of individual tubeholes (which constitute the
 37 assessment points located on the TP), and an estimate for a component-level
 280 probability *PoIC*. The latter was then used to infer the numbers of tubeplates
 within a plant population which, according to the probabilistic assessment, are
 expected to have at least one instance of creep-fatigue initiation on any tubehole
 surface.

285 For this case-study, the performance function is prescribed by the R5 Volume
 2/3 procedure, which defines the underlying deterministic set of calculations
 which map a plethora of material and loading input parameters onto the desired
 output (in this case creep-fatigue damage after a predefined period of in-service
 operation). Providing a detailed account of the underlying assessment proce-
 290 dure is beyond the purposes of this paper, however interested readers should

Table 1: Summary of the input parameters that were treated stochastically in the probabilistic R5 Vol 2/3 assessment of the TP component [29]. Material properties are temperature dependent, and the quoted values are given at $550^{\circ}C$ for reference. For lognormal parameters, the medians and coefficients of variation (CoV) are for the $\log_{10}(x)$ transformation of each parameter.

Parameter Description	Units	Probabilistic representation	Median (CoV)
Young's modulus (E)	GPa	Normal	158 (0.063)
Proof stress (S_y)	MPa	Normal	162 (26)
Constant in the <i>Ramberg-Osgood</i> expression (A)	MPa	Normal	1648 (210)
Coefficient of thermal expansion (α)	$\frac{1}{^{\circ}C} \times 10^{-6}$	Normal	20 (0.0359)
Creep ductility (ε_f)	mm/mm	Lognormal	1.029 (0.29)
Creep strain rate ($\dot{\varepsilon}_C$)	$1/hr$	Lognormal	- (0.3805)
Cycles to fatigue failure (N_f)	Cycles	Lognormal	-
Steady-operation stress (σ_{SO})	MPa	Histograms	-
Steady-operation metal temperature (T_{SO})	$^{\circ}C$	Histograms	-
Start-up & reactor-trip stresses (σ_{SU} & σ_{RT})	MPa	Histograms	-256 & 300
Start-up & reactor-trip metal temperatures (T_{SU} & T_{RT})	$^{\circ}C$	Histograms	436 & 363

refer to the R5 documentation [5], whilst [26] provides tutorials on procedure implementation, and application examples can be found in [7, 9, 16, 27, 28].

3.2. Results and Discussion

3.2.1. Deterministic Damage Results

295 Conducting deterministic calculations is an initial stage of developing a probabilistic assessment. In this work, a deterministic assessment assumes all input

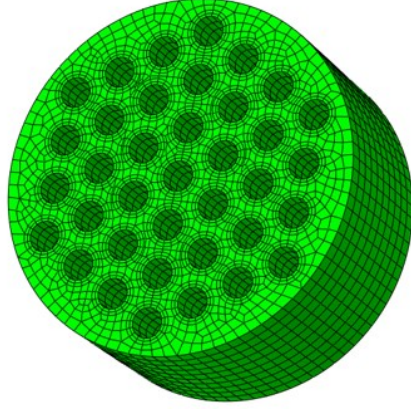


Figure 2: Finite element representation of the tubeplate with the 37 tubeholes being the key assessment locations [10].

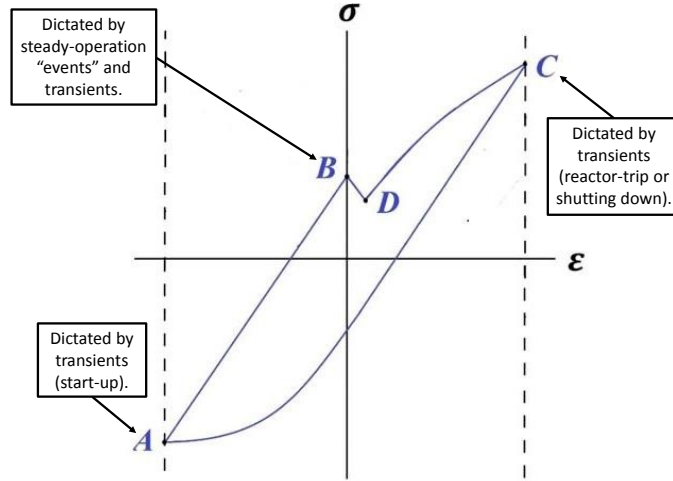


Figure 3: Schematic of a typical stress-strain (σ - ϵ) hysteresis cycle for a point located on the surface of a tubehole going through a reactor-trip to start-up (RT-SU) cycle. Points A and C are associated with SU and RT transients respectively [10].

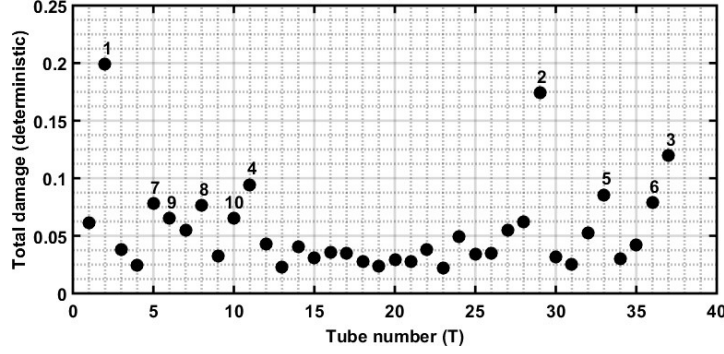


Figure 4: Total damage results of all 37 tubeholes using the deterministic (all parameters fixed at median values) assessment. The numbers indicate the order of the most damaged tubeholes from highest to lowest total damage.

parameters are set at their median values. All 37 TP tubeholes were examined and the deterministic damage results are shown in Figure 4. Whilst all tubeholes' damages were less than unity, it is apparent that a number of tubeholes incurred substantially larger damages than others; tubeholes 2 and 29 had the most severe damages. For clarity, all assessment results (deterministic and probabilistic) are associated with a specific point on the surface of each tubehole. Therefore, the damages shown in Figure 4 are associated with what are believed to be the most damaged points on each tubehole. The deterministic results could perpetuate a misleading belief that assessment locations which do not incur damages larger than unity will have zero *PoI*. However, a probabilistic mindset would reject such notion as the deterministic calculations do not account for the degree of scatter in the inputs as well as the output damage. Accordingly, a small damage does not always translate to a zero *PoI*. However, typically it should be expected that the tubeholes which have larger damages would also be the most probable to initiate. Thus the deterministic damages give some insight into which tubeholes to prioritise when conducting assessments, which relates to the discussion on dominant assessment locations.

3.2.2. Probabilistic Damage Results

For a single assessment point, Figure 5 shows a histogram of the total creep-fatigue damage obtained from the N number of MCS trials conducted. The constituents of the total damage are also presented separately to show that creep dominates the total damage, D_T , as indicated by the fatigue damage being comparatively small. Thereafter, the probability of initiation was calculated as $PoI = \frac{m}{N}$, where m is the number of initiations. The PoI of individual assessment locations can be tracked as the simulated history progresses, which is depicted in Figure 6. Logically, for some initial period, no initiations occur, but once initiations start an initial jump would be expected, which is the trend observed in Figure 6. As discussed later, creep ductility and deformation are two dominant inputs, and the substantial jumps at the start were attributed to MCS trials which had fast creep rates and/or small ductilities, as these would be expected to initiate first. After these early groups of crack initiations, the subsequent increase in the PoI was gradual which mirrors the progressive accumulation of damage. Convergence was also investigated, with Figure 7 showing an example of the convergence of the PoI where the uncertainty can be estimated using Eq 3. This highlights the fact that the estimated PoI is a random output, as it always has a degree of uncertainty which depends on the number of trials. For later calculations which involve component and population-level estimates (e.g. PoI_C and N_{CC}), an analysis can be conducted to assess their sensitivity towards the uncertainty in the PoI of individual assessment points. A small number of assessment points usually dominate the component-level probability and, therefore, it would be expected that estimating the uncertainties associated with these dominant points would suffice. However, such analysis was not considered as part of this case-study.

3.2.3. Sensitivity Analysis Results

A number of calculations were conducted to assess the sensitivity of the output damage results towards various input conditions. Firstly, sensitivity measures were calculated using the four approaches detailed in [9] to assess the

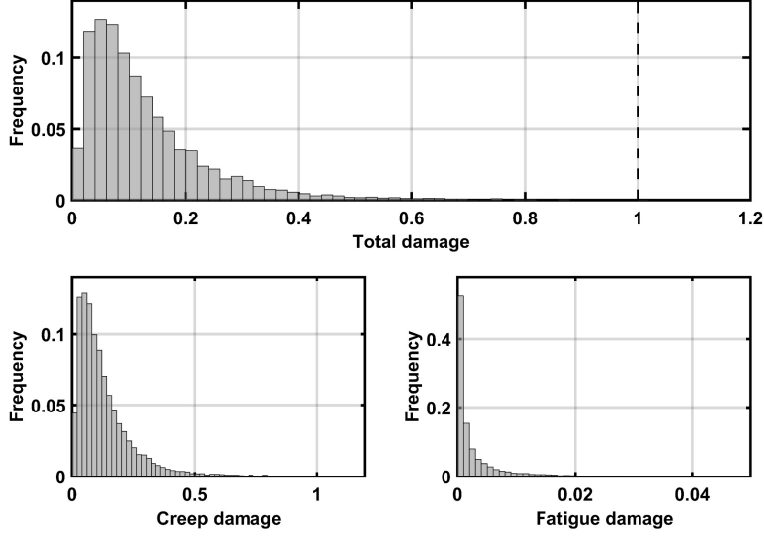


Figure 5: Example histograms of probabilistic damage results for a single assessment location. The criterion for creep-fatigue crack initiation is defined by $D_T \geq 1$ which also dictates the PoI (see Eq. 2). To clarify, there are some data at damages above 1, but too few to be visible on these histograms.

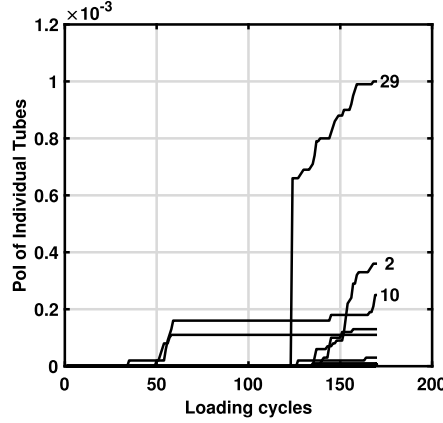


Figure 6: The evolution of the PoI for individual tubeholes during the simulated history (≈ 170 loading cycles), with each line representing the results from a MCS per tubehole. The three most probable tubeholes to initiation a crack were 29, 2, and 10 as labelled.

dominance (i.e. relative importance) of all stochastic inputs. The easiest of the
 345 four approaches is the correlations based method, as it can be conducted with

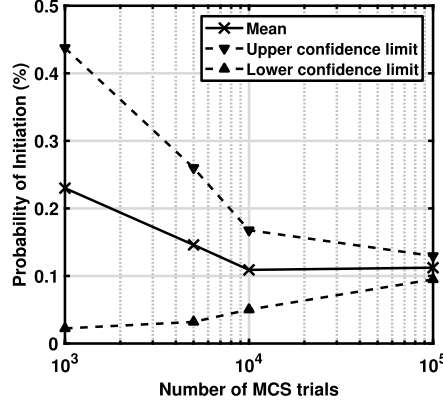


Figure 7: Convergence of the *PoI* prediction for an individual assessment location (tubehole 29). The uncertainty (i.e. upper-lower limits associated with a 95% confidence interval) can be estimated using Eq 3.

the results from a single MCS run by calculating the correlations between the inputs and the output damage. The simplicity of this method is particularly useful in the development stage of a probabilistic assessment. The complete set of quantitative SA results is shown in Figure 8, which indicate that creep ductility and deformation dominate the probabilistic damage results. This is consistent with the observations in [9] which looked at a similar but much simpler creep-fatigue assessment.

In this work all input parameters were assumed to follow specific probability distribution types (mostly either normal or lognormal). However, the SA results presented in Figure 8 can provide focus for investigating whether better statistical representations of some input parameters are likely to yield significant changes in the results. With creep ductility (ϵ_f) being a crucial input, it was judged important to investigate the effect of using different parameter distributions. The following is a discussion of the benefit of using a three-parameter probability distribution which incorporates a minimum value (x_0) in its probability density equation. Figure 9 shows two PDFs for ductility, one of which uses a 3-parameter formulation. The overall effect on the output damage PDF

was modest, however, using a 3-P lognormal resulted in a lower estimate for the PoI as highlighted in Table 2. Including a minimum value is logical within the context of ductility, as it is a positive non-zero quantity and the tail of the distribution is defined by a minimum value. Given the strong influence of ductility on the assessment results, it is compelling that including a minimum value can non-trivially reduce the estimated PoI . Furthermore, these observations corroborate the results in Figure 8 by indicating that changes in the way creep ductility is modelled can significantly affect the estimated PoI . Though this was not investigated, it is expected that the use of a more complex ductility models incorporating strain-dependency would produce substantial benefits (i.e. reduction in estimated damage) and is suggested as future work.

As previously discussed, assessing sensitivity can also be done with respect to the various assumptions involved in the underlying assessment. When conducting a creep damage assessment a judgement needs to be made as to whether creep strain (though not creep damage) resets at the start of each loading cycle (i.e. full primary reset, PR) or whether it continuously aggregates throughout the loading history (full continuous hardening, CH). The former assumption produces larger damages because more time is spent in the primary creep stage (which is characterised by faster creep strain rates) as a fraction of the simulated lifetime. Typically PR is more appropriate when there is significant reverse plasticity at the end of each creep dwell. Most commonly though, a real situation is somewhere in between, as some cycles might lead to full primary reset due to large plasticity while others might unload elastically. A model has been recently developed to model the amount of creep strain re-priming as a function of plastic strain, which is termed the ζ_P model for creep hardening [30], though it is still under development. Figure 10 shows the probabilistic damage results for a single tubehole, which shows the effect of using the three available options for creep hardening. As expected, there is a significant difference between using PR and CH, with the former producing larger damages, and by extension larger probabilities of initiation. Comparing the results for PR and the ζ_P model in-

Table 2: Comparisons between the *PoIs* from two assessments using two-parameter (2-P) and three-parameter (3-P) configurations of the lognormal distribution for the input creep ductility (ε_f).

Assessment location	PoI (2-P)	PoI (3-P)
Tube 2	1.0×10^{-3}	0.6×10^{-3}
Tube 29	1.4×10^{-3}	1.3×10^{-3}

dicates that assuming PR is not excessively conservative and is closer the ζ_P situation which is believed to be more realistic. This is a result of significant reverse plasticity being incurred which has been confirmed separately from the hysteresis cycle construction. The main conclusions from this analysis are that the assessment results are sensitive to the choice of hardening assumption and trialling with the ζ_P model provided valuable insight as to which assumption is more appropriate. The results indicate that PR is an acceptable assumption for assessing the TP, while incorporating the ζ_P model would be of limited benefit. Noteworthy is that the results presented in this work were all obtained using PR, unless otherwise stated.

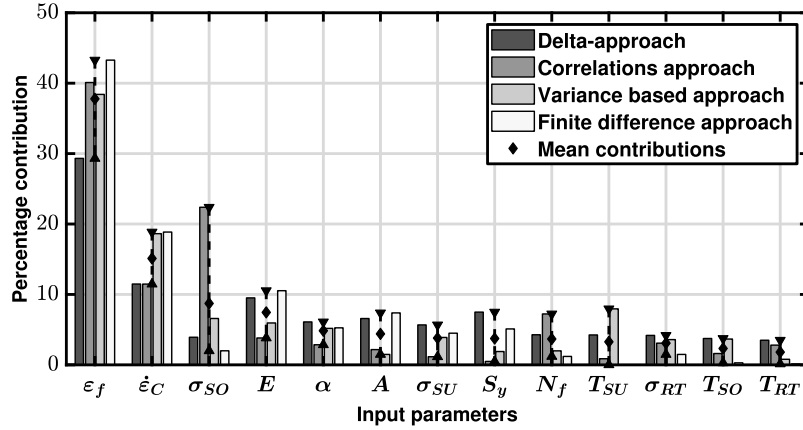


Figure 8: Sensitivity measures based on four approaches showing the comparative influence 13 stochastic inputs towards the probabilistic damage results for a single assessment point.

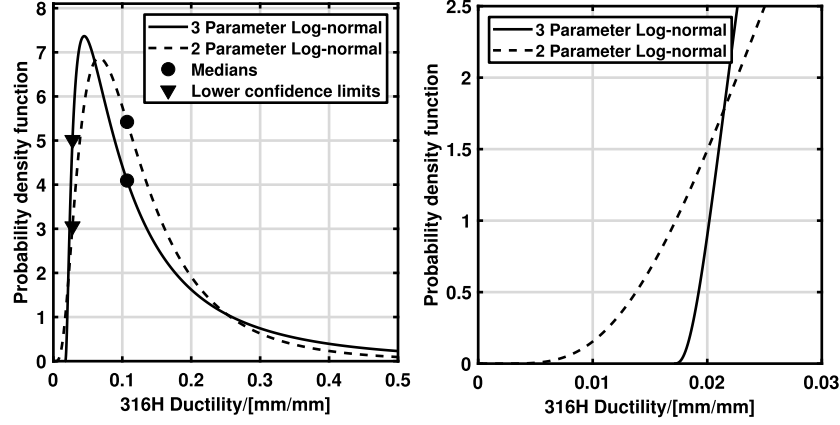


Figure 9: Shown on the left is a comparison between using 2 and 3 parameter formulations of the lognormal distribution for modelling the uncertainty in creep ductility (ϵ_f). The two distributions have identical medians and lower-bounds. On the right is a zoomed-in view of the tails of the fitted distributions, highlighting that the 3 parameter lognormal provides more control over the location of the tail.

3.2.4. Component-Level Results

Based on the methods discussed in Section 2.6, PoI_C (the probability of having at least one crack initiation in the whole TP) can be estimated from the PoI_s of individual tubeholes. The tubeholes which dominate PoI_C can be identified by counting the number of times each tubehole led to the first crack initiation. For the TP, the percentage number of times that each dominant tubehole led to cracking is shown in Figure 11, which provides a quantitative measure of dominance. Thereafter, PoI_C was calculated using Eq 6, which assumes the independence of the non-dominant assessment locations but uses PoI_{JC} as the *joint* probability for the dominant ones. As a result, Eq 6 assumes *partial* independence of the assessment locations. An estimate for PoI_C was also calculated using Eq. 4, which assumes *complete* independence of all tubeholes, and therefore is more conservative. A summary of these results is shown in Table 3. Furthermore, to assess the collective influence of the non-dominant tubeholes (31 out of 37 tubeholes), PoI_C was also calculated with and without their contribution as detailed in Table 3. These results suggest that such influence

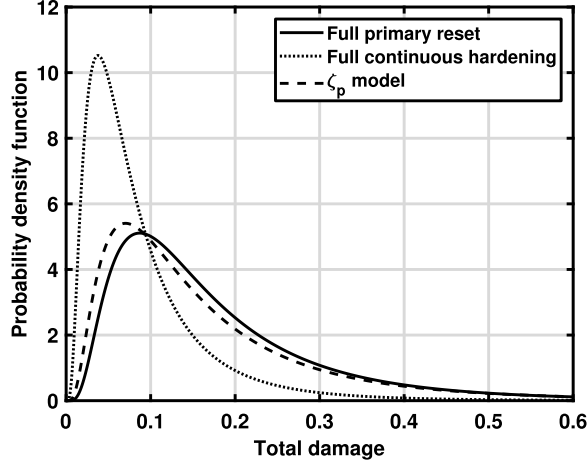


Figure 10: Comparison between probabilistic results using three assumptions for creep hardening.

is rather subtle. Finally, the best estimate for PoI_C was 0.19% which accounts for all tubeholes and assumes partial independence.

3.2.5. Population-Level Results

Based on PoI_C a prediction can be made as to the number of components which have at least one crack initiation (N_{CC}) given a population of N_{TC} components. All components are assumed to be identical and have the same PoI_C and, therefore, N_{CC} follows a binomial distribution prescribed by Eq. 7. Note that this is not physically indicative for a real plant case, where some components will be less severely stressed or cycled than others. Therefore, the calculations herein are for illustration only, and will bound the real situation. Figure 12 shows the binomial PDF and CDF using $PoI_C = 0.19\%$ and $N_T = 128$ which is the total number of tubeplates in operation. One way to interpret these results is by examining an upper-bound value of N_{CC} (e.g. the 95% value), which in this case is 1. This means that there is approximately a 95% probability of $N_{CC} \leq 1$.

Taking a different perspective, what can also be of interest is the approximation of an acceptable PoI_C by the end of service given a target upper-bound

Table 3: Comparison of estimates of the component-level probability of initiation (PoI_C) based on assuming complete versus partial independence of the individual tubeholes, and based on considering the dominant tubeholes only (see Figure 11) versus all tubeholes.

Independence	PoI_C in %	
	Dominant tubeholes only	Including all tubeholes
Complete	0.19	0.22
Partial	0.16	0.19

N_{CC} , which can be demanded by safety regulations. For the TP, to ensure a probability of at least 95% that N_{CC} is zero, then $PoI_C < 0.04\%$ must be achieved, while for $N_{CC} = 1$ a range of $0.04\% \leq PoI_C < 0.26\%$ must be demonstrated for the same minimum confidence level. These ranges follow from the binomial distribution being discreet in nature, which only provides probabilities for integer values of N_{CC} and, as there exists a range of PoI_C values that would yield the same upper-bound N_{CC} . Hence these ranges ensure a confidence limit of 95% or larger.

4. CONCLUSION

This paper introduces a complete methodology which can be translated to any structural integrity application, whilst giving a high-temperature creep-fatigue example for contextualisation and demonstrating the implementation of the methodology. Systematic probabilistic methods and concepts were incorporated, the most prominent of which are: Monte-Carlo Simulations, latin-hypercube sampling, sensitivity analysis, correlations between input parameters, treatment of loading uncertainties and the extrapolation to component and population-level estimates.

Probabilistics must not be considered an alternative to conventional deterministic calculations, but rather a completely different mindset which embraces complexity and uncertainty rather than simplifying them in favour of conser-

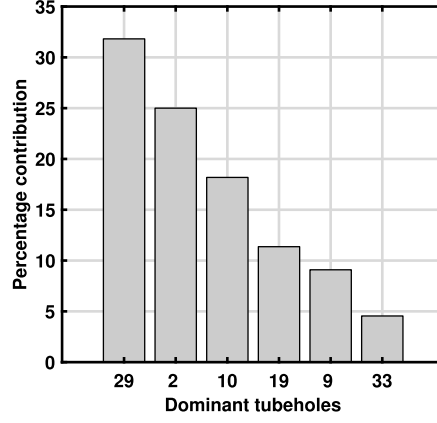


Figure 11: A breakdown of the percentage number of times each of the dominant tubeholes led to the first crack initiation across the whole tubeplate.

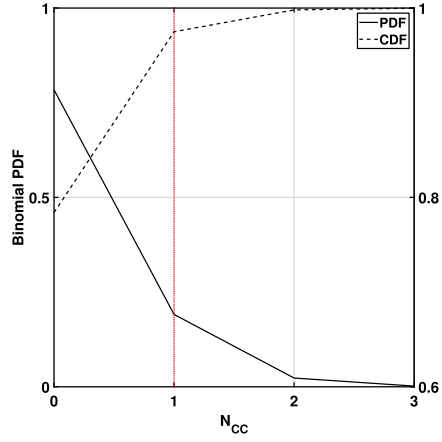


Figure 12: Binomial distribution (see Eq. 7) for a population of components of $N_{TC} = 128$ given that $PoI_C = 0.19\%$. The solid line (PDF) is the probability of having exactly the stated number of cracked tubeplates across the fleet of 128. The dashed line (CDF) represents the probability of having N_{CC} cracked tubeplates or fewer. The dotted vertical line denotes the 95% upper limit, highlighting the upper-bound value for N_{CC} , which in this case indicates that there is a 95% probability of there existing 1 cracked tubeplate or less.

1
2
3
4
5
6
7
8
9
10
11
12
13
14
15
16
17
18
19
20
21
22
23
24
25
26
27
28
29
30
31
32
33
34
35
36
37
38
39
40
41
42
43
44
45
46
47
48
49
50
51
52
53
54
55
56
57
58
59
60
61
62
63
64
65

vatism. Accordingly, probabilistics can be considered an evolution of tradi-
460 tional deterministic approaches, which have emerged from the reconciliation
of statistical methods and physics of failure modelling, aided by advances in
computational tools and hardware. In general, for implementing probabilistic
methodologies within structural integrity there are three facets of knowledge
required [12]:

- 465 1. Understanding of the underlying physics of failure and data for the statis-
tical characterisation of material property inputs.
2. Operational data for components of interest.
3. A general appreciation of probabilistic approaches and statistical concepts
and the ability to relate these to a physical problem of interest.
- 470 4. Computational experience in producing efficient algorithms.

These sources of knowledge can be aggregated into probability estimates of hi-
erarchical elements: individual assessment points within a component, a whole
component and a population of components. Consequently, the implementation
of probabilistic approaches is intended to provide more confidence in assessment
475 procedures and results, and their utilities are especially pronounced for plant
applications, where complexity is translatable to statistical and probabilistic
paradigms.

The vision for this work is to bridge the gap between the knowledge of
480 probabilistic methods and the general structural integrity community. Moving
forward, substantial thought must be devoted to bringing practitioners up to a
baseline level of understanding and awareness of probabilistic and statistical con-
cepts. This will also have the benefit of continuously developing the prospective
probabilistic structural integrity methodology through feedback on use, valida-
485 tion and independent verification. By promoting further implementation and
engagement, it is envisaged that the methodology will mature and emerge to
be more extensive as well as coherent, which in turn will aid further acceptance
within a wide range of structural integrity fields and, therefore, promoting the

emergence of a unified probabilistic framework for structural integrity.

ACKNOWLEDGEMENTS

The authors would like to express their gratitude for the support of EDF Energy towards this project and in particular Dr Marc Chevalier.

REFERENCES

- [1] P. M. James, J. K. Sharples, N. Underwood, UK programme on codes, standard and procedure needs for SMR and Gen IV reactors, Proceedings of the ASME 2018 Pressure Vessels & Piping Conference. Codes and Standards, PVP2018-85075, July 2018.
- [2] American Society for Mechanical Engineers, ASME III Rules for Construction of Nuclear Facility Components-Division, Division 1, Subsection NH, Class 1, Components in Elevated Temperature Service (2015).
- [3] AFCEN, RCC-MRx - Design and Construction Rules for Mechanical Components of Nuclear Installations (2015).
- [4] British Standards Institution, BS 7910 - Guide to Methods for Assessing the Acceptability of Flaws in Metallic Structures (2013).
- [5] EDF Energy Nuclear Generation Ltd, R5 Issue 3 Volume 2/3 (Rev.002): Creep-Fatigue Crack Initiation Procedure for Defect-Free Structures. Assessment Procedure for the High Temperature Response of Structures (Nov 2014).
- [6] J. Sharples, P. Budden, Recent developments associated with the R6 defect assessment methodology, Transactions of the 22rd International Conference on Structural Mechanics in Reactor Technology, SMiRT-22, San Francisco, California, USA, Aug 2013.

- [7] M. J. Chevalier, The Reliability of Degrading Structural Systems Operating at High Temperature, Ph.D. thesis, University of Bristol, Bristol, United Kingdom (Mar 2013).
- [8] H. Conlin, P. G. Brabazon, K. Lee, Exploring the Role and Content of the Safety Case, Process Safety and Environmental Protection 82 (4) (2004) 283 – 290.
- [9] N. A. Zentuti, J. D. Booker, R. A. W. Bradford, C. E. Truman, A review of probabilistic techniques: towards developing a probabilistic lifetime methodology in the creep regime, Materials at High Temperatures 34 (5-6) (2017) 333–341.
- [10] N. A. Zentuti, J. D. Booker, R. A. W. Bradford, C. E. Truman, Management of complex loading histories for use in probabilistic creep-fatigue damage assessments, Proceedings of the ASME 2018 Pressure Vessels & Piping Conference. Codes and Standards, PVP2018-84400, 2018.
- [11] N. A. Zentuti, J. D. Booker, R. A. W. Bradford, C. E. Truman, Correlations between creep parameters and application to probabilistic damage assessments, International Journal of Pressure Vessels and Piping 165 (2018) 295 – 305.
- [12] N. A. Zentuti, J. D. Booker, J. Hoole, R. A. W. Bradford, D. Knowles, Probabilistic structural integrity, The UK Form for Engineering Structural Integrity (FESI) Bulletin: Vol. 12, Issue 2 (Winter 2018), pp. 16–23.
- [13] Y. M. Goh, The Incorporation of Uncertainty into Engineering Knowledge Management, Ph.D. thesis, University of Bristol, Bristol, United Kingdom (Jan 2005).
- [14] Y. M. Goh, C. A. McMahon, J. D. Booker, Improved utility and application of probabilistic methods for reliable mechanical design, Proceedings of the Institution of Mechanical Engineers, Part O: Journal of Risk and Reliability 223 (3) (Sep 2009) 199–214.

- [15] Y. M. Goh, J. Booker, C. McMahon, A Comparison of Methods in Probabilistic Design Based on Computational and Modelling Issues, Springer Netherlands, Dordrecht, 2005, pp. 109–122.
- [16] R. A. W. Bradford, A Procedure for Probabilistic Creep-Fatigue Crack Initiation Assessment Consistent With R5 Volume 2/3, Tech. Rep. E/REP/BBAB/0028/GEN/13, EDF Energy Nuclear Generation Ltd (Jan 2014).
- [17] B. Dogan, U. Ceyhan, J. Korous, F. Mueller, R. Ainsworth, Sources of scatter in creep/fatigue crack growth testing and their impact on plant assessment, *Welding in the World* 51 (7) (2007) 35–46.
- [18] J. D. Booker, M. Raines, K. G. Swift, Designing Capable and Reliable Products, Butterworth-Heinemann, 2001.
- [19] K. Bury, Statistical Distributions in Engineering, Cambridge University Press, 1999.
- [20] M. C. Cario, B. L. Nelson, Modelling and generating random vectors with arbitrary marginal distributions and correlation matrix, Delphi Packard Electric Systems (Warren, OH) and Department of Industrial Engineering and Management Science, Northwestern University, Evanston IL (1997).
- [21] Matworks, Generate Correlated Data Using Rank Correlation, URL: <https://uk.mathworks.com/help/stats/generate-correlated-data-using-rank-correlation.html>, accessed May 30, 2017 (2017).
- [22] F. Pianosi, K. Beven, J. Freer, J. W. Hall, J. Rougier, D. B. Stephenson, T. Wagener, Sensitivity analysis of environmental models: A systematic review with practical workflow, *Environmental Modelling & Software* 79 (2016) 214–232.
- [23] E. Borgonovo, A new uncertainty importance measure, *Reliability Engineering & System Safety* 92 (6) (2007) 771–784.

- [24] P. Dillström, F. Nilsson, 7.11 - Probabilistic Fracture Mechanics, in:
I. Milne, R. Ritchie, B. Karihaloo (Eds.), Comprehensive Structural Integrity, Pergamon, Oxford, 2003, pp. 465 – 489.
- [25] N. A. Zentuti, Plant data analysis for incorporation of loading uncertainties in probabilistic damage assessments, Tech. rep., University of Bristol, Solid Mechanics Research Group on behalf of EDF Energy Nuclear Generation Limited (Sep 2018).
- [26] R. A. W. Bradford, T73S04 Creep-Fatigue Crack Initiation Tutorials, URL: <http://rickbradford.co.uk/T73S04Tutorials.html>, accessed Dec 07, 2018 (2015).
- [27] Z. Fan, D. J. Smith, X. Chen, M. W. Spindler, Creep-fatigue lives prediction and sensitivity study of 316h at 550°C, Acta Metallurgica Sinica (English letters) 24 (2) (2011) 132–140.
- [28] R. Bradford, P. Holt, Application of probabilistic modelling to the lifetime management of nuclear boilers in the creep regime: Part 2, International Journal of Pressure Vessels and Piping 111-112 (2013) 232–245.
- [29] EDF Energy Nuclear Generation Ltd, AGR Materials Data Handbook, R66, Issue 6, Rev.010 (Nov 2016).
- [30] E. F. J. Shelton, HTBASS Creep Understanding: Re-Priming of Creep Deformation Behaviour During Cyclic Loading, Tech. Rep. 5147229/301/002: Issue 02, prepared by Atkins on behalf of EDF Energy Nuclear Generation Ltd (Oct 2016).